

Improved Low Voltage Ride-Through Strategy for Grid-Connected Photovoltaic Systems during Line-to-Line Fault

Mokabbera Billah, *Graduate Student Member, IEEE*, Shameem Ahmad, *Member, IEEE*, Chowdhury Akram Hossain, *Senior Member, IEEE*, Md. Rifat Hazari, *Member, IEEE*

Abstract—With the increasing integration of photovoltaic (PV) systems into power grids, Low Voltage Ride-Through (LVRT) capability has become crucial for maintaining grid stability and reliability. Existing LVRT strategies often struggle with asymmetrical faults, leading to DC-link voltage fluctuations and inadequate reactive power support. This study proposes an improved integrated control method to enhance the LVRT capability of grid-tied PV systems during asymmetrical disturbances. The control strategy integrates DC-link voltage regulation, reactive power injection, and voltage sag compensation, considering both balanced and unbalanced fault conditions. A PI controller with cascaded control with feed-forward decoupling in the current loop is implemented for improved current control, while a Synchronous Reference Frame Phase-Locked Loop (SRF-PLL) ensures grid synchronization. This integrated approach offers advantages in system stability, rapid fault response, and grid code compliance. Simulation results for a 1.5 MW PV plant demonstrate the control's effectiveness, reducing grid voltage sag by 96.5%, injecting up to 78% of reactive power, and maintaining DC-link voltage within acceptable limits during Line-to-line faults.

Index Terms—Asymmetrical faults, DC-link voltage regulation, Grid stability, Low voltage ride through, Reactive power injection.

I. INTRODUCTION

QUICK integration of renewable energy sources particularly photovoltaic (PV) systems into the utility grid has caused grid operators to face significant challenges in maintaining a reliable and constant power supply [1]. A considerable problem is guaranteeing grid-tied solar systems' LVRT capabilities during grid disruptions, particularly during asymmetrical faults. These disruptions may induce significant voltage swings, potentially resulting in the disconnection of photovoltaic inverters from the grid. The abrupt cessation of power generation from photovoltaic systems during such situations

might intensify the disruption, potentially instigating cascading failures and jeopardizing the integrity of the whole power system [3]. Grid operators and regulatory authorities have instituted rigorous LVRT standards, obligating grid-tied PV systems to maintain functionality and deliver reactive power assistance during grid disruptions, such as asymmetrical faults. These criteria frequently delineate the reactive power injection patterns essential for voltage restoration during diverse fault scenarios [4]. Noncompliance with LVRT regulations may disrupt the power supply from photovoltaic systems to the utility grid, resulting in significant financial losses and potentially causing widespread blackouts. This highlights the necessity of formulating effective control techniques to improve the LVRT capabilities of grid-interactive PV systems, especially during asymmetrical faults.

Recent research has highlighted the challenges posed by asymmetrical faults in PV systems, with a particular emphasis on enhancing LVRT capabilities using proportional-integral (PI) control strategies. Asymmetrical faults, which result in unbalanced voltage sags, present unique control challenges compared to symmetrical faults [5]. For a three-phase grid-tied PV system during asymmetrical failures, the PI-based control approach is developed [6], employing decoupled current regulation in positive and negative sequence frames. While this improved power quality and reduced harmonics, it didn't adequately address DC-link voltage fluctuations under severe unbalanced conditions. A PI control with a feed-forward compensation method designed to reduce power oscillations during asymmetrical faults [7]. This improved dynamic and steady-state performance but struggled to adapt to varying fault depths. Addressing the challenge of reactive power injection during unbalanced faults, [8] developed a modified PI controller with an adaptive gain scheduling mechanism.

Their approach allowed for flexible reactive current injection based on the severity of voltage sags in each phase, demonstrating improved voltage support capabilities. However, the transition between normal and fault operation modes remained a concern. To manage DC-link voltage during asymmetric faults, [9] suggested a PI control structure with two loops. They efficiently suppressed DC-link voltage fluctuations under unbalanced grid situations by using an inner current control loop and an outside voltage control loop. While effective, this approach did not fully integrate reactive power support requirements specified by grid codes. Recent work by [10] focused on optimizing PI controller parameters for LVRT

Mokabbera Billah is with the Department of EEE, American International University-Bangladesh, Dhaka, Bangladesh (e-mail: 23-92927-1@student.aiub.edu).

Shameem Ahmad is with the Department of EEE, BSRM School of Engineering, BRAC University, Dhaka, Bangladesh (e-mail: shameem.ahmad@bracu.ac.bd).

Chowdhury Akram Hossain is with the Department of Computer Engineering, American International University-Bangladesh, Dhaka, Bangladesh (e-mail: chowdhury.akram@aiub.edu).

Md. Rifat Hazari is with the Department of EEE, American International University-Bangladesh, Dhaka, Bangladesh (e-mail: rifat@aiub.edu).

during asymmetrical faults. They employed a particle swarm optimization algorithm to tune PI gains, achieving improved transient response and steady-state performance. However, their method required offline optimization, limiting real-time adaptability to changing fault conditions. While these advancements have significantly improved the performance of PI-based controllers during asymmetrical faults, challenges remain in developing a comprehensive control approach that simultaneously addresses multiple objectives. Most existing strategies focus on specific aspects such as current control [11] or reactive power injection [12], often at the expense of other critical parameters like DC-link voltage stability.

This research introduces an innovative combined control technique to improve the LVRT capabilities of grid-tied single-stage PV systems during asymmetrical fault scenarios. The suggested control seeks to address the deficiencies of current methodologies by concurrently combining numerous control objectives, such as DC-link voltage management, overvoltage reduction, and reactive power injection during diverse grid disturbances. The proposed approach improves the LVRT performance of grid-tied PV systems by integrating techniques for DC-link voltage regulation, DC-DC converter control, and grid code-compliant reactive power injection while ensuring adherence to grid codes and maintaining system stability and reliability during various fault conditions. This work's primary contributions are:

- To develop a control strategy that addresses asymmetrical fault conditions in grid-tied PV systems.
- To implement a DC-link voltage regulation and overvoltage mitigation strategies during power imbalances, to maintain power balance between the utility grid and PV arrays under various fault types.
- To design a reactive power injection control system that meets grid code specifications for maintaining voltage during asymmetric failures.

The following parts are structured as outlined below: The architecture of the analyzed grid-tied photovoltaic system, encompassing system design, components, and low-voltage ride-through requirements, is detailed in section II. The third part presents the simulation results and examines the control's performance. The work is concluded in Section IV, which also offers some possible avenues for future investigation.

II. SYSTEM MODELING AND COMPONENT DESCRIPTION

A. Grid Code Requirements

LVRT capability is essential for grid-tied renewable energy systems, ensuring that producing units stay connected during transient voltage reductions resulting from faults or disruptions. International grid codes delineate diverse LVRT stipulations, as seen in Fig. 1.

The ENTSO-E rules of the European Union stipulate that units must endure voltage reductions of 15% for 150

milliseconds, but the FERC Order No. 661-A in the United States mandates that wind turbines must stay connected during 15% voltage dips for 625 milliseconds. China's rules mandate that wind power facilities must function at voltage reductions of 20% for a duration of 625 milliseconds [13]. The Central Electricity Authority (CEA) of India requires units to endure voltage reductions of 15% for a duration of 300 milliseconds. The Energy Commission of Malaysia rules that units must stay connected during 15% voltage dips for 200 milliseconds, whereas the Bangladesh Power Development Board (BPDB) requires devices to endure 20% voltage decreases for 150 milliseconds. These varied needs underscore the global significance of LVRT capabilities in preserving grid stability and dependability across multiple power systems.

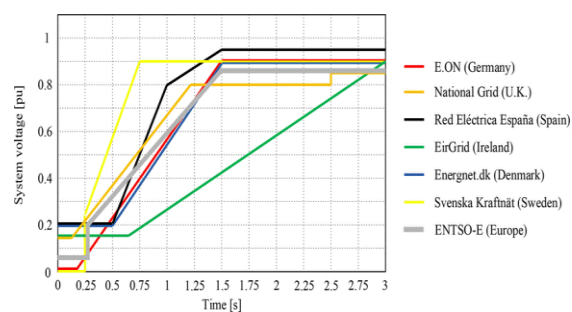


Fig. 1. LVRT requirements in International Grid Codes [14]

The ENTSO-E rules of the European Union stipulate that units must endure voltage reductions of 15% for 150 milliseconds, but the FERC Order No. 661-A in the United States mandates that wind turbines must stay connected during 15% voltage dips for 625 milliseconds. China's rules mandate that wind power facilities must function at voltage reductions of 20% for a duration of 625 milliseconds [13]. The Central Electricity Authority (CEA) of India requires units to endure voltage reductions of 15% for a duration of 300 milliseconds. The Energy Commission of Malaysia rules that units must stay connected during 15% voltage dips for 200 milliseconds, whereas the Bangladesh Power Development Board (BPDB) requires devices to endure 20% voltage decreases for 150 milliseconds. These varied needs underscore the global significance of LVRT capabilities in preserving grid stability and dependability across multiple power systems.

B. Modeling of grid-tied PV System

Grid-compatible power is produced from solar energy using a grid-tied PV system. Direct current electricity produced by the solar array is converted into alternating current power by a sequence of electronic converters and filters [15]. A capacitor maintains a steady DC voltage while the DC-DC converter modifies the solar array voltage and current [16]. After converting DC electricity to AC power using Pulse Width Modulation, the inverter routes the AC power through a transformer to meet the grid level [17]. The basic modeling of grid-connected photovoltaic systems is shown in Fig. 2. The specifications of the proposed system are displayed in Table 1.

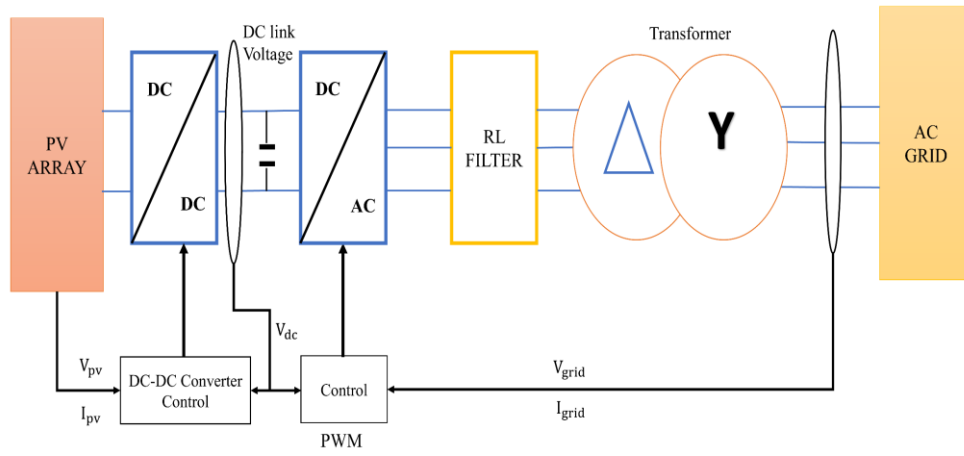


Fig. 2. Modeling of a grid-tied PV system

C. Photovoltaic Module and Array

To accurately analyze a PV module's electrical behavior, an equivalent circuit model is vital. This enables precise performance prediction and effective system design. The single-diode equivalent circuit is the most widely used model, offering a good balance of simplicity and accuracy for most applications [18].

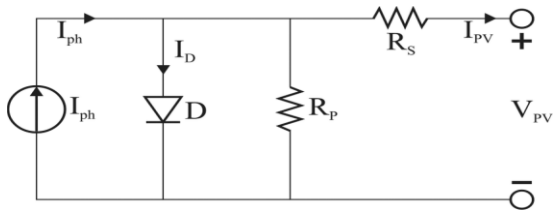


Fig. 3. PV equivalent Circuit [19]

This model features a current source I_{ph} representing light-generated photocurrent, connected in parallel with a diode simulating the solar cell's p-n junction. To account for non-idealities and losses, a series of resistance R_s and a parallel resistance R_p are included. Fig. 3 depicts this equivalent circuit model of the PV system, which provides a comprehensive representation for detailed analysis of solar energy systems. The mathematical model presented in this research establishes the relationship between the output voltage and current of a photovoltaic (PV) module. It also provides a method for calculating the photocurrent generated under specific environmental conditions [20]. The electrical behavior of a PV module can be characterized by a set of equations [21].

$$I_L = I_{PH} - I_{sat} \left(e^{\frac{qV_d}{mN_sKT}} - 1 \right) - \frac{I_L R_s + V_L}{R_p} \quad (1)$$

$$I_{PH} = [I_{sc} + \alpha_i (T - T_{ref})] \frac{G}{G_{ref}} \quad (2)$$

$$I_{sc} = I_{sc,ref} \left(\frac{R_p + R_s}{R_p} \right) \quad (3)$$

$$I_{sat} = \frac{[I_{sc,ref} + \alpha_i (T - T_{ref})]}{\left(e^{\frac{q(V_{oc,ref} + \alpha_v (T - T_{ref}))}{mN_sKT}} \right) - 1} \quad (4)$$

The study validates the power-voltage (P-V) and current-voltage (I-V) characteristics of PV modules through simulations conducted under standard test conditions, specifically at a reference temperature of $T_{ref} = 25^\circ\text{C}$ and irradiance of $G_{ref} = 1000 \text{ W/m}^2$. Table I presents the specifications of the grid-tied PV system, PV module, and PV array.

TABLE I
SPECIFICATIONS OF PV MODULE AND PV ARRAY [21]

Parameters	The value
Grid Voltage	33 kV
Grid frequency	50 Hz
Transformer	0.4/33kV
DC Link Voltage	800 V
Maximum-power-current	8.04 A
Maximum-power-voltage	49.78 V
Open-circuit-current	8.56 A
Open-circuit-voltage	60 V
Parallel & series resistance	389.9 Ω , 0.33 Ω
Maximum-power	400 W

This study simulated a 1.5 MW_p grid-tied photovoltaic power plant utilizing MATLAB/Simulink software. The array design is optimized to attain a harmonious balance between voltage and current requirements for grid integration. The array has 235 parallel strings, each consisting of 16 modules interconnected in series via [18],[21]. The specified configuration yields a peak power point current (I_{mpv}) of 1889.4 A and a peak power point voltage (V_{mpv}) of 796.4 V, resulting in a DC output power of 1504718.1 W under standard testing circumstances. The open-circuit voltage (V_{PV-oc}) of the array is 960 V, while the short-circuit current (I_{PV-sh}) is rated at 2011.6 A. The identification of these parameters is crucial for determining the performance attributes of the array and for developing appropriate power conditioning devices for grid integration.

D. DC-Link Voltage Regulation

One crucial element of the proposed control scheme, intended to guarantee steady operation in both normal circumstances and grid disturbances, is DC link voltage

management. This control supersedes the traditional Maximum Power Point Tracking (MPPT) technique, delivering improved performance amongst network fluctuations. The control employs a Proportional-Integral (PI) control structure, as seen in Fig. 4, which illustrates the suggested control circuit. The control's principal functions are to sustain voltage overshoot, manage energy transfer from the solar array to the grid inverter, and enhance system resilience during grid variations. The regulator ensures a steady power flow, enhancing energy conversion efficiency and optimizing overall system performance. It also plays a crucial role in maintaining stability during grid anomalies, guaranteeing reliable operation of the grid-tied PV system.

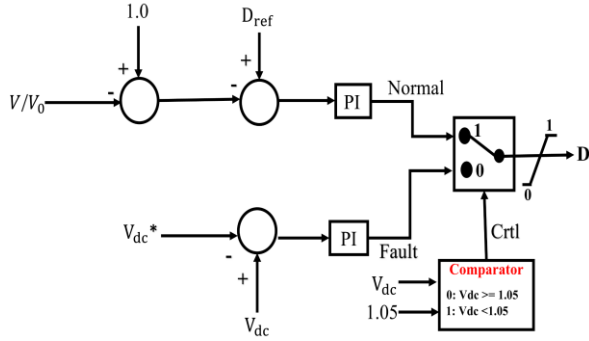


Fig. 4. DC-link Voltage Control Circuit [22]

The control law is given by:

$$u(t) = K_p * e(t) + K_i * \int e(t)dt \quad (5)$$

Where, $u(t)$ = Control signal (duty cycle for the boost converter), $e(t)$ = Error signal (difference between reference and measured DC-link voltage), K_p = Proportional gain, K_i = Integral gain.

The control continuously monitors the voltage across the V_{dc} and compares it to a reference value V_{dc_ref} . A preset threshold, usually set at 1.05 per unit, is exceeded by the V_{dc} , at which point the control kicks in to regulate the voltage levels. The actual DC-link voltage is measured as part of the control method, which also involves calculating the error $e(t) = V_{dc_ref} - V_{dc}$ and applying the Proportional-Integral (PI) control rule to produce the control signal $u(t)$ and the controllers were tuned using trial and error method and the PI controller values are shown in Table II. The control signal is then used to adjust the boost converter's duty cycle, which successfully raises the DC-link voltage to the desired amount.

E. Modeling of Grid Inverter

In grid-tied PV systems, the VSI is a crucial component that makes power conversion easier. By connecting the PV system to the electrical grid, the system ensures that all applicable grid requirements are followed. An exterior voltage control loop and an internal current control loop are components of the inverter's architecture [16]. The DC side voltage is controlled by the external voltage control loop, which typically maintains between 50 to 850 V [23]. This system's DC-link voltage is set at 800 V, which is not too far from the PV array's maximum

output voltage of 796.4 V. Fig. 5 shows the schematic design of the inverter control working under typical circumstances. To keep the inverter operating at a unity power factor, the inner current control loop modifies the grid current. This satisfies grid standards requiring a power factor higher than 0.9 in either a leading or lagging fashion. The DC-link voltage must be controlled and stabilized by the outside control loop. To enable improved control capabilities, a feed-forward decoupling controller is used to differentiate between the active and reactive current components. A Synchronous Reference Frame Phase-Locked Loop is implemented to achieve grid synchronization [17]. The pulse-width modulation signal generator uses the outputs of the voltage and current control loops to create reference voltages by converting them from the dq0 reference frame to the abc frame. These switching pulses control how the inverter operates. The grid inverter's output voltages can be stated as follows:

$$V_{ia} = L \frac{di_a}{dt} + Ri_a + V_{ga}$$

$$V_{ib} = L \frac{di_b}{dt} + Ri_b + V_{gb} \quad (6)$$

$$V_{ic} = L \frac{di_c}{dt} + Ri_c + V_{gc}$$

Where i_a , i_b , and i_c are inverter output currents, V_{ia} , V_{ib} , and V_{ic} are inverter output voltages, and V_{ga} , V_{gb} , and V_{gc} are grid voltages. Applying a rotational synchronous d-q reference frame transformation:

$$V_{id} = L \frac{di_d}{dt} + Ri_d + V_{gd} \quad (7)$$

$$V_{iq} = L \frac{di_q}{dt} + Ri_q + V_{gq} \quad (8)$$

The active and reactive power equations in space vector notation are:

$$P = \frac{3}{2}(V_{gd}I_d + V_{gq}I_q) \quad (9)$$

$$Q = \frac{3}{2}(-V_{gd}I_q + V_{gq}I_d) \quad (10)$$

During normal operation, with a balanced system and neglecting power losses, setting the q-axis voltage (V_q) to zero ensures unity power factor operation. This simplifies the power equations:

$$P = \frac{3}{2}V_{gd}I_d \quad (11)$$

$$Q = -\frac{3}{2}V_{gd}I_q \quad (12)$$

These formulas demonstrate that the d-axis current (I_d) alone controls the active power, whereas the q-axis current (I_q) controls the reactive power.

F. Modeling of Proposed LVRT Control

Fig. 6 shows the recommended LVRT control. Under fault conditions, the control approach is used to keep the DC-link voltage within allowable bounds. In the synchronous reference frame, the reference values for the direct and quadrature current

components (I_d^* and I_q^*) are calculated [24]. Proportional-integral (PI) controllers are used to compare the reference and actual currents. Based on this comparison, the controller generates the necessary control signals that allow the inverter to maintain synchronization with the utility grid and regulate the output currents. Fig. 5 shows inverter control during normal conditions.

The control strategy includes a defect detection approach that observes voltage sags or dips, which may signify possible disruptions or problems in the system. Control signals are changed based on the fault state (no fault or fault) to mitigate the impact of faults and maintain stable operation. Table II presents the K_p and K_i values of the PI controllers of the Inverter, which were determined through a trial-and-error approach.

The control approach utilizes Pulse-Width Modulation (PWM) techniques and dq/abc coordinate transformations for accurate control and efficient power conversion [21],[24]. These algorithms generate appropriate switching signals for the inverter, assuring stability and optimizing power quality [22].

TABLE II
SPECIFICATIONS OF PI CONTROLLERS

PI Controllers	K_p Value	K_i Value
PI ₁	0.5	10
PI ₂	1.2	50
PI ₃	0.3	5
PI ₄	0.4	8
PI ₅	1.2	50
PI ₆	1.5	60
PI ₇	0.8	20

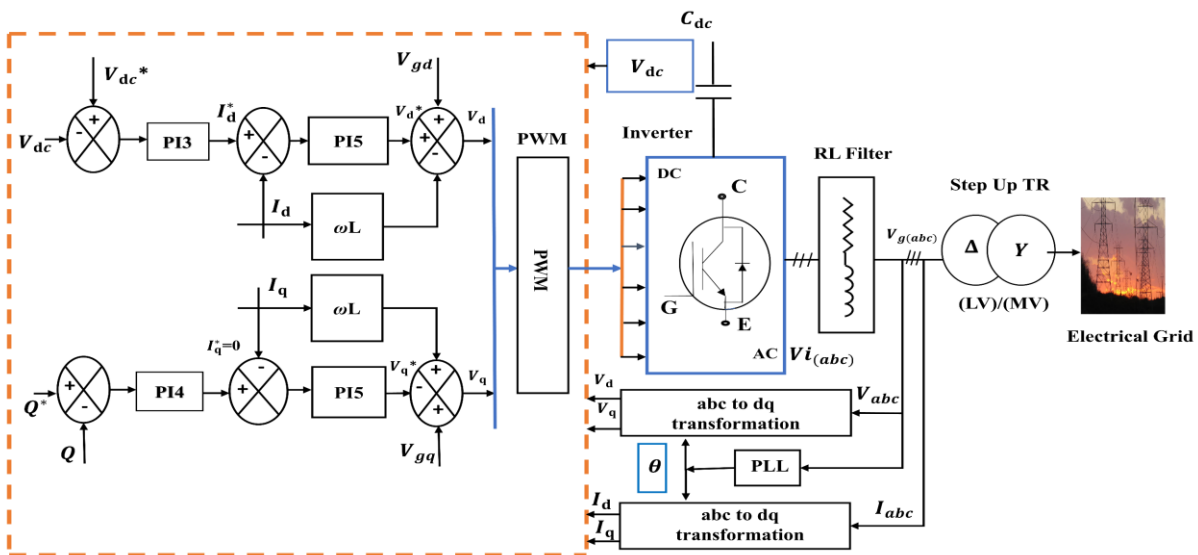


Fig. 5. Schematic of the voltage source inverter side control during normal conditions

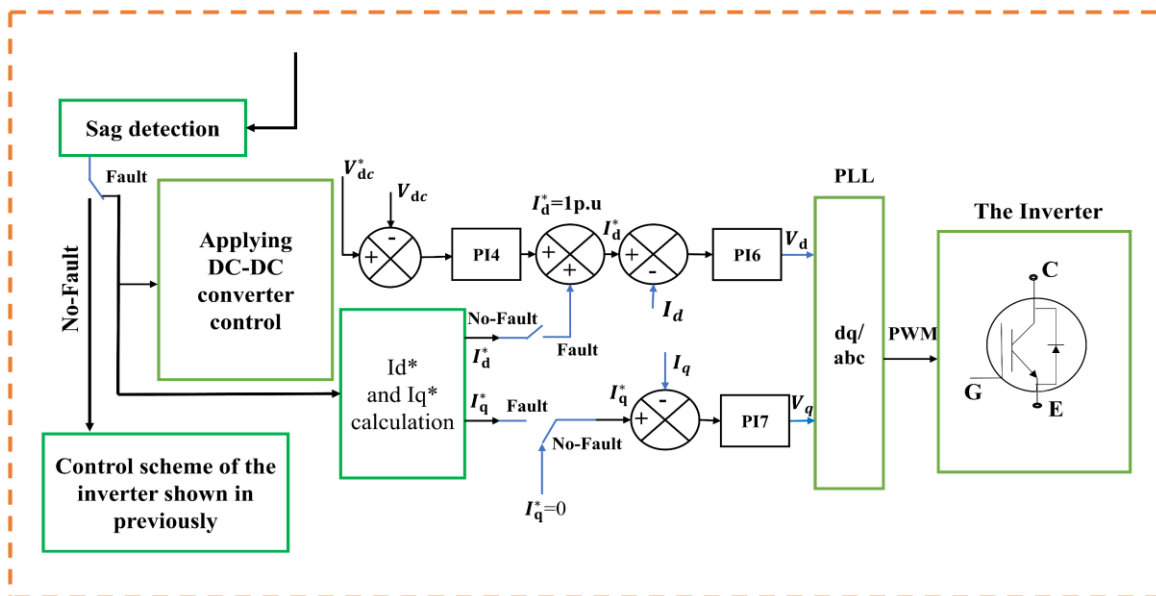


Fig. 6. Schematic of proposed unified LVRT control

III. RESULT ANALYSIS

For a grid-interactive PV system, MATLAB/Simulink simulations were used to assess the efficacy of the suggested LVRT control approach. Asymmetrical fault scenarios are recognized as a crucial situation for grid-tied systems and were simulated for a 1.5 MW PV plant. Fig. 7 shows the Simulink model. The simulation's outcomes showed how well the suggested LVRT control worked to keep the PV array functioning dependably even during an asymmetrical fault. The simulation was run for 9s, and the fault was created at 4s and was cleared after 1s, which is 5s.

Fig. 8 and Fig. 9 show the DC link voltage during a fault situation. Without the DC link control in Fig. 8, the voltage overshoot is up to 2500 volts. However, with the control in Fig. 9, the overshoot is mitigated, and the voltage is within an acceptable limit. Fig. 10 and Fig. 11 show the inverter voltage response during the asymmetrical fault. Fig. 10 (rms) and Fig. 12 (sinusoidal) show that without the LVRT control, the voltage sag is almost 50%. But Fig. 11 (rms) and Fig. 13 (sinusoidal) show that with the LVRT control, the voltage sag is compensated up to 96.23%. Fig. 14 and Fig. 16 show the grid voltage response during the asymmetrical fault. Fig. 14 (rms) and 16 (sinusoidal) show that without the LVRT control, the voltage sag is almost 50%. But Fig. 15 and Fig. 17 show that with the LVRT control, the voltage sag is compensated up to 96.5%.

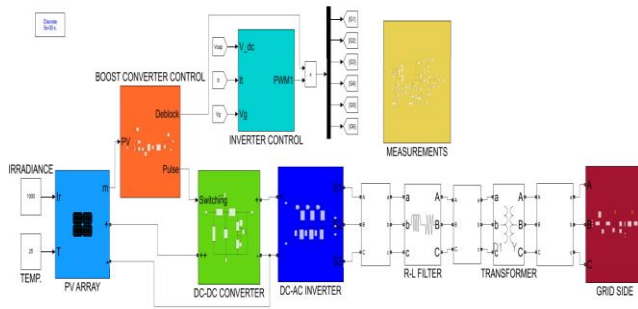


Fig. 7. Simulink model of proposed LVRT control method

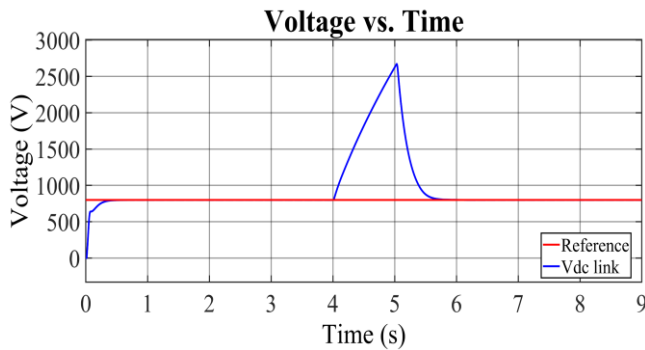


Fig. 8. DC link Voltage without the proposed DC-DC control method

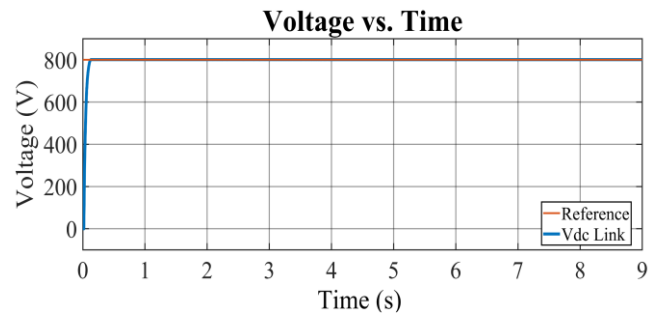


Fig. 9. DC link voltage with proposed DC-DC control method

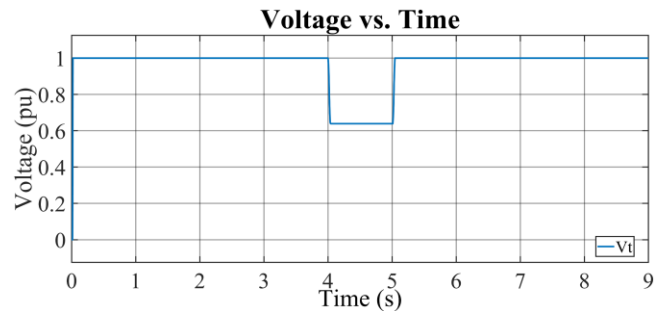


Fig. 10. Inverter voltage (rms) without LVRT Control

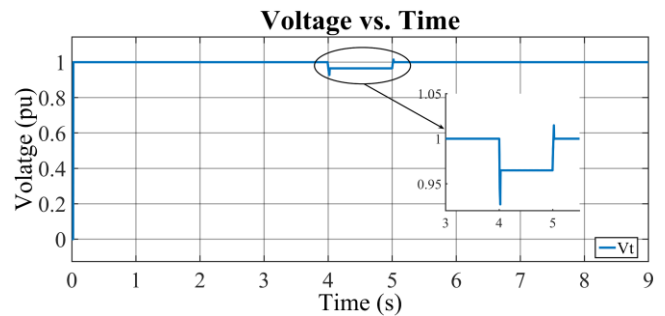


Fig. 11. Inverter voltage (rms) with proposed LVRT Control

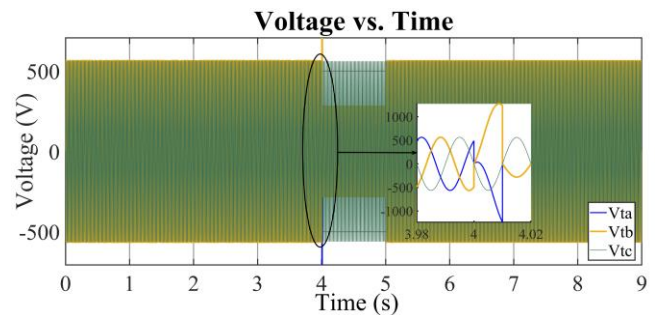


Fig. 12. Inverter voltage (sinusoidal) without LVRT Control

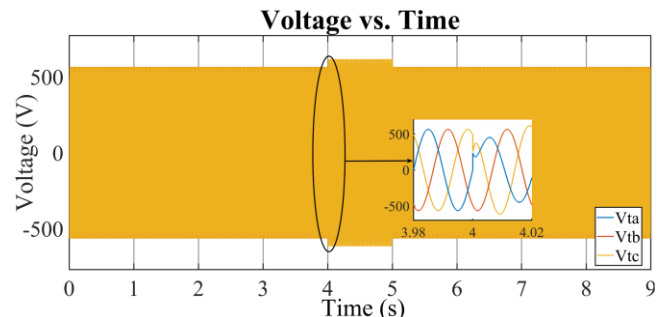


Fig. 13. Inverter voltage (sinusoidal) with proposed LVRT Control

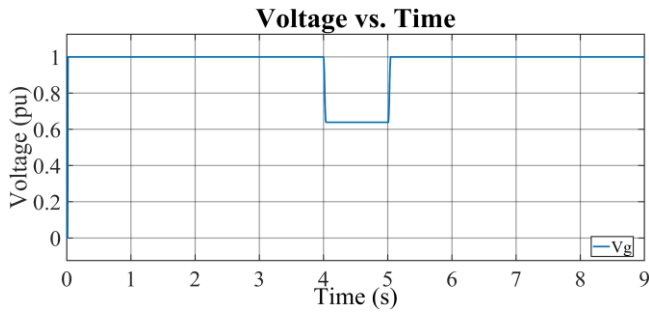


Fig. 14. Grid voltage (rms) without LVRT Control

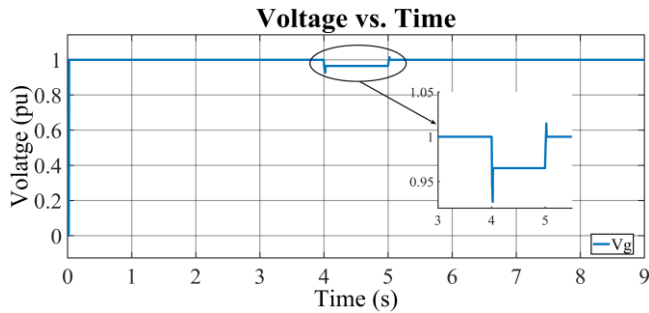


Fig. 15. Grid voltage (rms) with proposed LVRT Control

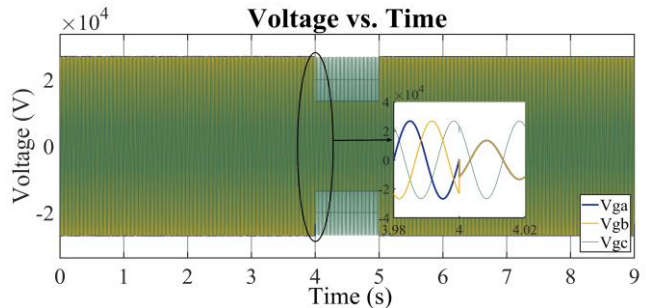


Fig. 16. Grid voltage (sinusoidal) without LVRT Control

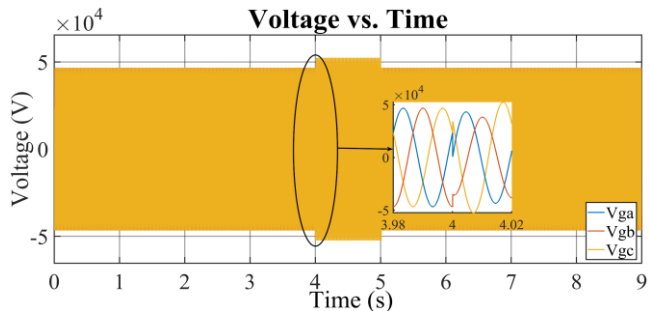


Fig. 17. Grid voltage (sinusoidal) with proposed LVRT Control

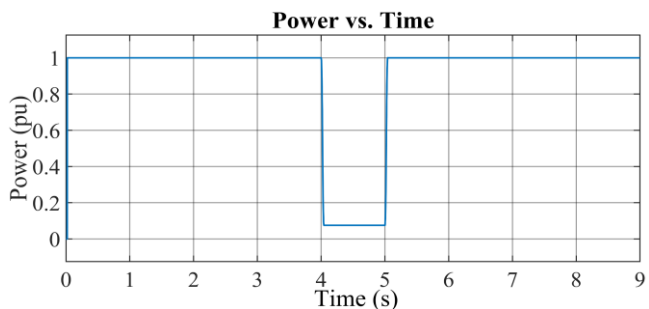


Fig. 18. Real Power during line-to-line fault with proposed LVRT method

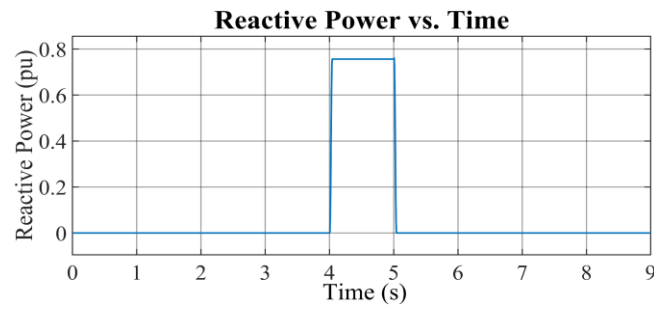


Fig. 19. Reactive Power during line-to-line fault with proposed LVRT method

Fig. 18 and 19 show the active power and reactive power response during the asymmetrical fault respectively. Fig. 18 shows that during the fault, the power is dropped to 50%. Fig.19 demonstrates that up to 78% of the reactive power is injected during the fault. Power grids, and following the fault clearing, the maximum active power and the lowest reactive power are reached.

The findings indicate that in the absence of the suggested LVRT control strategy, these systems face challenges in sustaining stable operation and in recovering voltages to their pre-fault levels within the timeframe mandated by grid codes. The suggested LVRT control strategy presents multiple significant advantages. Initially, it reduces DC-link overvoltage, efficiently averting excessive voltage accumulation in the DC-link that might otherwise harm system components.

Furthermore, the control system adds reactive power to the grid during voltage dips, helping to stabilize the grid and improve overall stability. The approach guarantees uninterrupted fault ride-through by facilitating smooth functioning during asymmetrical fault occurrences and permitting a swift transition back to normal operations once the fault is resolved. Additionally, it manages voltage levels, ensuring that grid voltages remain within acceptable parameters during and following fault occurrences. The control ensures adherence to LVRT requirements outlined by grid interconnection standards, allowing the system to withstand low-voltage events.

Table III compares four control methods for handling asymmetrical faults in power systems: PI+BFCL, SD+BFCL, PI+DC Chopper, and a Proposed Control with PI. The comparison evaluates DC Link Voltage behavior, Grid Voltage recovery, Inverter voltage recovery, and Reactive power injection. The proposed control with PI demonstrates superior performance in DC Link Voltage, showing no spikes pre- or post-fault, while other methods experience various oscillations. It also achieves the highest Grid Voltage recovery at 96.5%, compared to 94% (SD+BFCL), 92% (PI+DC Chopper), and 90% (PI+BFCL), with some methods showing spikes. Only the proposed method reports Inverter voltage recovery at 96.23%. For Reactive power injection, both the PI+DC Chopper and the proposed method inject sufficient amounts, while this information is not provided for BFCL-based methods.

TABLE III
COMPARATIVE ANALYSIS BETWEEN DIFFERENT LVRT METHODS

Methods	PI+BFCL	SD+BFCL	PI+DC Chopper	Proposed Control with PI
Aspects				
Fault type	Asymmetrical	Asymmetrical	Asymmetrical	Asymmetrical
DC Link Voltage	Small oscillations during pre-fault & post-fault	Small oscillations during pre-fault & post-fault	Oscillation during pre-fault & post-fault	No spike during pre- or post-fault
Grid Voltage recovery	90% with spikes	94% with spikes	92%	96.5%
Inverter voltage recovery	Not mentioned	Not mentioned	Not mentioned	96.23%
Reactive power injection	Not mentioned	Not mentioned	Sufficient amount is injected	Sufficient amount is injected

The results of the simulation validate the effectiveness of the proposed LVRT control approach. The system showcases its capability to uphold stability, control voltages, and satisfy LVRT criteria across different fault scenarios. This performance underscores the strategy's ability to improve the reliability and grid integration features of PV systems.

IV. CONCLUSIONS

Specifically aimed at asymmetrical fault scenarios, a unified LVRT control method for grid-tied PV systems has been designed and assessed in this work. To guarantee grid code compliance and preserve system stability, the suggested control strategy includes several goals, including reactive power injection, overvoltage mitigation, and DC-link voltage management. The efficiency of the control system for a 1.5 MW PV plant was verified under Line-to-line fault situations using comprehensive modeling and MATLAB/Simulink simulations. Significant gains in voltage stability are shown by the findings, which show that the suggested control reduces grid voltage sag by 96.5%, injects up to 78% of reactive power, and avoids excessive DC-link overvoltage.

This method significantly improves the LVRT performance of PV systems connected to the grid. By injecting reactive electricity and maintaining voltage levels, the method not only guarantees ongoing power generation during grid disruptions but also maintains grid stability. In addition, the control method guarantees fault recovery with ease and complies with international grid norms, supporting grid dependability and renewable energy integration.

Future research could explore real-time adaptive algorithms for further optimizing controller performance under varying fault conditions and dynamic grid environments, paving the way for even more robust PV system integration into modern power grids.

REFERENCES

[1] S. Ahmad, H. Mubarak, U. K. Jhuma, T. Ahmed, S. Mekhilef, and H. Mokhlis, "Point of Common Coupling Voltage Modulated Direct Power Control of Grid-Tied Photovoltaic Inverter for AC Microgrid

Application," *Int. Trans. Electr. Energy Syst.*, vol. 2023, no. 1, Art. no. 3641907, 2023.

[2] T. J. Rumky, T. Ahmed, M. Ahmed, S. Ahmad, and M. M. Rahman, "Performance of microgrid systems on multiple dynamic loads penetration," in *Proc. 10th IEEE Int. Conf. Power Syst. (ICPS)*, 2023, pp. 1-6.

[3] [3] Z. Hossain, S. Ahmad, U. K. Jhuma, S. Mekhilef, M. Mubin, H. Mokhlis, and T. Ahmed, "A Flexible Interconnection and Power Sharing Strategy For Two Autonomous Microgrid Systems," in *Proc. IEEE 6th Int. Conf. Comput., Commun., and Autom. (ICCCA)*, 2021, pp. 472-477.

[4] U. K. Jhuma, S. Mekhilef, S. Ahmad, J. Islam, J. R. Jesan, and M. M. Billah, "The Impact of Synchronous Generator on Voltage Sag Mitigation in Power System Network," in *Proc. IEEE 4th Int. Conf. Comput., Power and Commun. Technol. (GUCON)*, 2021, pp. 1-5.

[5] J. Rocabert, A. Luna, F. Blaabjerg, and P. Rodriguez, "Control of power converters in AC microgrids," *IEEE Trans. Power Electron.*, vol. 27, no. 11, pp. 4734-4749, Nov. 2012.

[6] A. Merabet, L. Labib, A. M. Y. M. Ghias, C. Ghenai, and T. Salameh, "Robust feedback linearizing control with sliding mode compensation for a grid-connected photovoltaic inverter system under unbalanced grid voltages," *IEEE J. Photovoltaics*, vol. 7, no. 3, pp. 828-838, May 2017.

[7] S. Abbasi, A. A. Ghadimi, A. H. Abolmasoumi, M. R. Miveh, and F. Jurado, "Enhanced control scheme for a three-phase grid-connected PV inverter under unbalanced fault conditions," *Electronics*, vol. 9, no. 8, Art. no. 1247, 2020.

[8] P. P. Dash and M. Kazerani, "Dynamic modeling and performance analysis of a grid-connected current-source inverter-based photovoltaic system," *IEEE Trans. Sustain. Energy*, vol. 2, no. 4, pp. 443-450, Oct. 2011.

[9] Y. Gu, W. Li, and X. He, "Frequency-coordinating virtual impedance for autonomous power management of DC microgrid," *IEEE Trans. Power Electron.*, vol. 30, no. 4, pp. 2328-2337, Apr. 2014.

[10] A. Mojallal and S. Lottifard, "Enhancement of grid connected PV arrays fault ride through and post fault recovery performance," *IEEE Trans. Smart Grid*, vol. 10, no. 1, pp. 546-555, Jan. 2017.

[11] X. Guo, X. Zhang, B. Wang, W. Wu, and J. M. Guerrero, "Asymmetrical grid fault ride-through strategy of three-phase grid-connected inverter considering network impedance impact in low-voltage grid," *IEEE Trans. Power Electron.*, vol. 29, no. 3, pp. 1064-1068, Mar. 2013.

[12] J. Miret, A. Camacho, M. Castilla, L. G. de Vicuña, and J. Matas, "Control scheme with voltage support capability for distributed generation inverters under voltage sags," *IEEE Trans. Power Electron.*, vol. 28, no. 11, pp. 5252-5262, Nov. 2013.

[13] State Grid Corporation of China, "Grid Code for Wind Power Generation," Beijing, 2011.

[14] N. Espinoza and O. Carlson, "Field-test of wind turbine by voltage source converter," *Wind Energy Sci.*, vol. 4, pp. 465-477, 2019.

[15] M. N. Tasnim, T. Ahmed, S. Ahmad, S. Mekhilef, and S. M. Ferdous, "Autonomous power management and control among interconnected standalone hybrid microgrids," in *Proc. 10th IEEE Int. Conf. Power Syst. (ICPS)*, 2023, pp. 1-6.

[16] S. Ahmad, U. K. Jhuma, M. Karimi, A. Pourdayaei, S. Mekhilef, H. Mokhlis, and K. Kauhaniemi, "Direct power control based on point of common coupling voltage modulation for grid-tied AC microgrid PV inverter," *IEEE Access*, vol. 10, pp. 109187-109202, 2022.

[17] S. Ahmad, S. Mekhilef, H. Mokhlis, M. Karimi, A. Pourdayaei, T. Ahmed, U. K. Jhuma, and S. Afzal, "Fuzzy logic-based direct power control method for pv inverter of grid-tied ac microgrid without phase-locked loop," *Electronics*, vol. 10, no. 24, Art. no. 3095, 2021.

[18] S. Bagchi, D. Chatterjee, R. Bhaduri, and P. K. Biswas, "An improved low-voltage ride-through (LVRT) strategy for PV-based grid connected inverter using instantaneous power theory," *IET Gener. Transm. Distrib.*, vol. 15, no. 5, pp. 883-893, 2021.

[19] M. N. Tasnim, T. Ahmed, M. A. Dorothei, S. Ahmad, G. M. Shafiqullah, S. M. Ferdous, and S. Mekhilef, "Voltage-oriented control-based three-phase, three-leg bidirectional AC-DC converter with improved power quality for microgrids," *Energies*, vol. 16, no. 17, Art. no. 6188, 2023.

[20] Y. Bak, J. S. Lee, and K. B. Lee, "Low-voltage ride-through control strategy for a grid-connected energy storage system," *Appl. Sci.*, vol. 8, no. 1, Art. no. 57, 2018.

[21] A. Q. Al-Shetwi, M. Z. Sujod, and F. Blaabjerg, "Low voltage ride-through capability control for single-stage inverter-based grid-connected photovoltaic power plant," *Sol. Energy*, vol. 159, pp. 665-681, 2018.

[22] S. I. Mahmud, M. A. Mannan, and M. R. Hazari, "Design and Performance Analysis of a PV Control Scheme to Improve LVRT of

Hybrid Power System," *AIUB J. Sci. Eng. (AJSE)*, vol. 20, no. 2, pp. 20-21, 2021.

- [23] T. Orłowska-Kowalska, F. Blaabjerg, and J. Rodriguez, Eds., *Advanced and Intelligent Control in Power Electronics and Drives*. Berlin, Germany: Springer, 2014.
- [24] M. Billah, S. Ahmad, M. R. Hazari, A. R. Sagor, T. Ahmed, S. Mekhilef, M. Seyedmahmoudian, A. Stojcevski, and O. Alshammari, "Integrated DC-link regulation and reactive power injection strategies for LVRT compliance of grid-tied PV systems," in *Proc. Int. Conf. Electr. Electron. Eng.*, 2024, pp. 503–519.



Mokabbera Billah (Graduate Student Member, IEEE) received her B.Sc. Engineering and M.Sc. Engineering degrees in Electrical and Electronics Engineering from American International University-Bangladesh in 2022 and 2024, respectively. Her research interests include microgrid operation control, power system stability, renewable energy integration with the grid, PV inverter control, LVRT, and FRT.



Shameem Ahmad (Member, IEEE) is an Associate Professor at the Department of Electrical and Electronic Engineering, BRAC University. From Universiti Malaya, Malaysia, in 2014 and 2022, he has received Master of Engineering Science and PhD in Electrical Engineering respectively. He received Bachelor of Engineering in Electrical and Electronic Engineering from Visvesvaraya Technological University, India, in 2009. Prior joining to BRAC University, he has taught in American International University-Bangladesh. He is an editorial board member and distinguished reviewer in prominent international journals published by IEEE, Elsevier, Wiley, Springer etc. He engages in industrial consultancy for major corporations on power system and renewable energy projects. His research interests include smart grid, microgrid, power system control, power converter control and application of artificial intelligence in power systems.



Chowdhury Akram Hossain (Senior Member, IEEE) received his B.Sc. degree in Electrical and Electronics Engineering (EEE) and M. Engg. Degree (with the honour of Summa Cum Laude) in Telecommunication from the American International University-Bangladesh (AIUB), Dhaka, in 2008 and 2010 respectively, and PhD Degree from Universiti Sultan Zainal Abidin, Malaysia, in 2024. In 2010, he joined as a Special Assistant under the Office of Student Affairs, and a Senior Lecturer for the Electrical and Electronic Engineering Department, under the Faculty of Engineering at AIUB, where he is currently serving as an Associate Professor & Head of Computer Engineering Department at AIUB. He is also the Deputy Director of Dr. Anwarul Abedin Institute of Innovations. His research interests are in the field of e-health, power engineering, wireless communication, renewable energy, smart grid, and Ad Hoc Networks.



Md. Rifat Hazari (Member, IEEE) received his B.Sc. Engg. and M.Sc. Engg. Degrees in Electrical and Electronic Engineering from American International University-Bangladesh (AIUB) in August 2013 and December 2014, respectively, and a Ph.D. Degree in Energy Engineering from Kitami Institute of Technology (KIT), Japan, in March 2019. He served as an Assistant Professor and Lecturer in the Electrical and Electronic Engineering department at AIUB. Currently, he is working as a Deputy Director of Dr. Anwarul Abedin Institute of Innovation, AIUB, and a Senior Assistant Professor in the Electrical and Electronic Engineering department at AIUB. He received the MINT (Academic Excellence) Award 2017 from KIT for outstanding research of the 2017 academic year, Best Paper Award in the Australasian Universities Power Engineering Conference 2017, Melbourne, Victoria, Australia, Best Presentation Award in the IEEJ Branch Convention 2017, Hakodate, Japan and Best Sustainable Development Goal (SDG) Posterity Award in 3rd International Conference on Robotics, Electrical and Signal Processing Techniques 2023, Dhaka, Bangladesh. He has published more than 60 articles in different journals and at international and national level conferences. He has been an invited speaker at many universities and workshops. His research interests are renewable energy systems (especially wind power & photovoltaic power systems), power system stability and control, microgrid and hybrid power systems, HVDC systems, analysis and control of rotating electrical machines.